Electronic Supplementary Material (ESI) for Physical Chemistry Chemical Physics.
This journal is © the Owner Societies 2018

Electronic Supplementary Information

A structural model of the hierarchical assembly of an amyloid nanosheet by an infrared probe technique

*Baohuan Jia, Ying Sun, Lujuan Yang, Yang Yu, Haoran Fan and Gang Ma**

Key Laboratory of Medicinal Chemistry and Molecular Diagnosis of Ministry of Education, Key Laboratory of Analytical Science and Technology of Hebei Province, College of Chemistry and Environmental Science, Hebei University, Baoding 071002, China

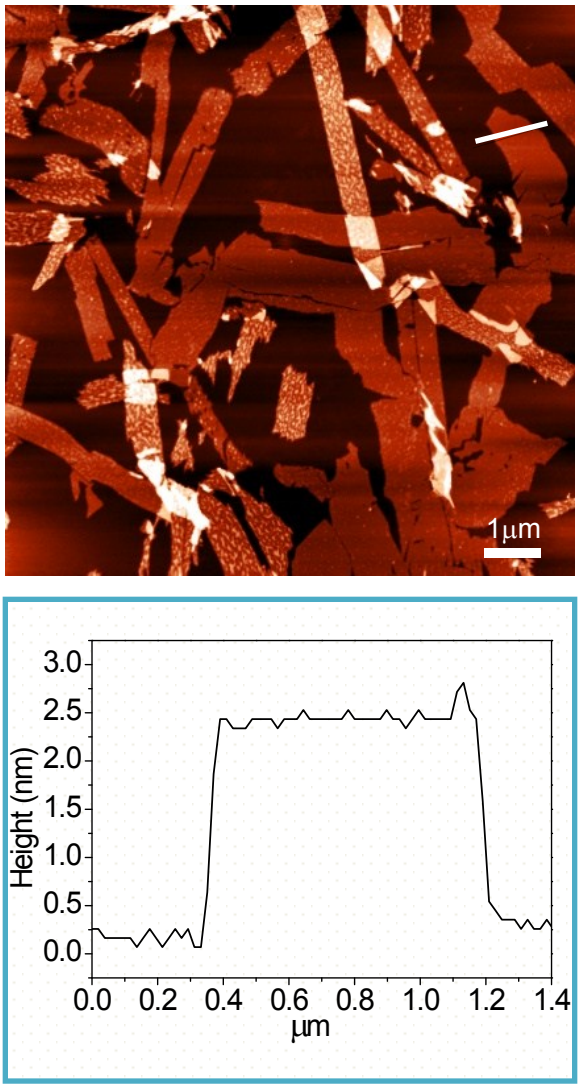

Figure S1. AFM morphology (top) and height (bottom) characterizations of the native KLVFFAK nanosheet.

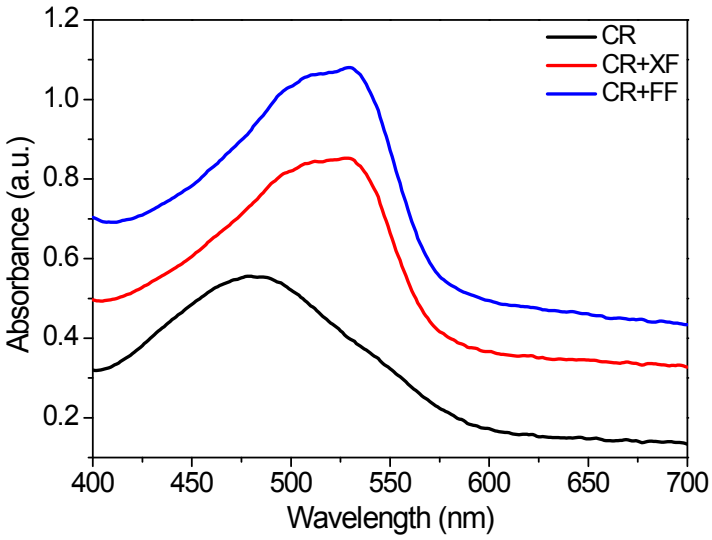

Figure S2. Congo red (CR) assay of the KLVXFAK nanosheet and the native KLVFFAK nanosheet. XF: KLVXFAK nanosheet; FF: KLVFFAK nanosheet. The two nanosheet spectra have been offset vertically for better display and their absorbance values are thus in arbitrary unit (a.u.). The baseline tilt in the two nanosheet spectra is due to nanosheet scattering.

Table S1. Curve-fitting analysis parameters in Figure 3

Peak Frequency (cm^{-1})	Amplitude (a.u.)	FWHM* (cm^{-1})	Line-shape
2237	0.17	11.0	Voigt
2231	0.79	7.00	Voigt
2227	0.35	5.32	Voigt

*FWHM: full width at half maximum.

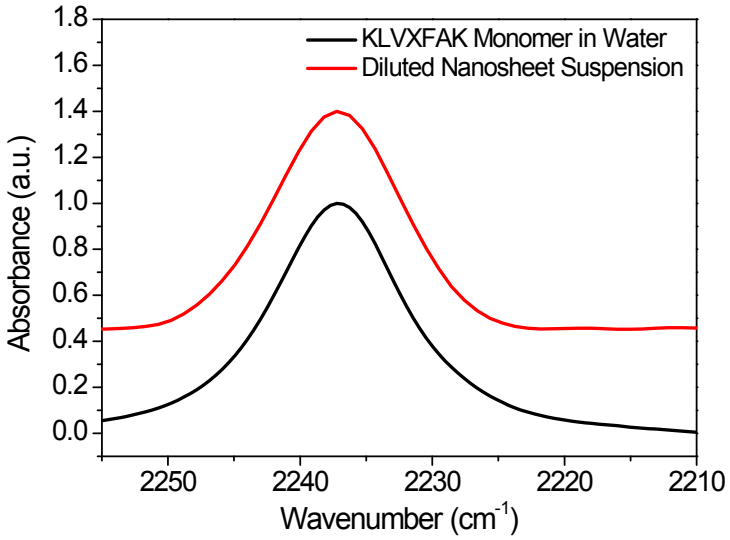

Figure S3. Comparison of the top spectrum in Figure 4 and the FTIR spectrum of the monomeric KLVXFAK peptide in water in the CN probe region.

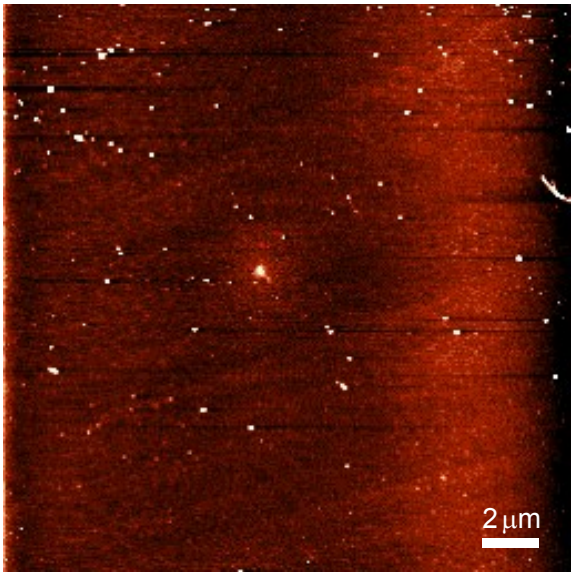

Figure S4. AFM morphology characterization of the KLVXFAK incubation solution at the very beginning of the incubation (t=0h).

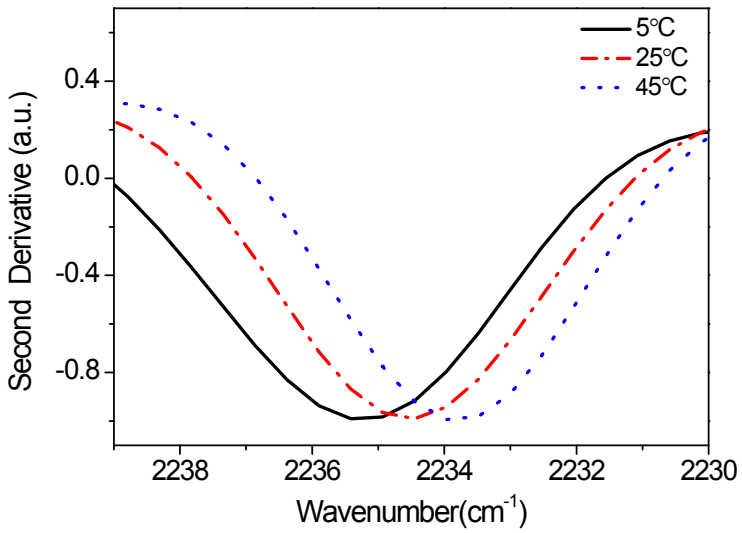

Figure S5. A) Temperature-dependent change of the second derivative spectra of the CN stretch of *p*-tolunitrile in water.

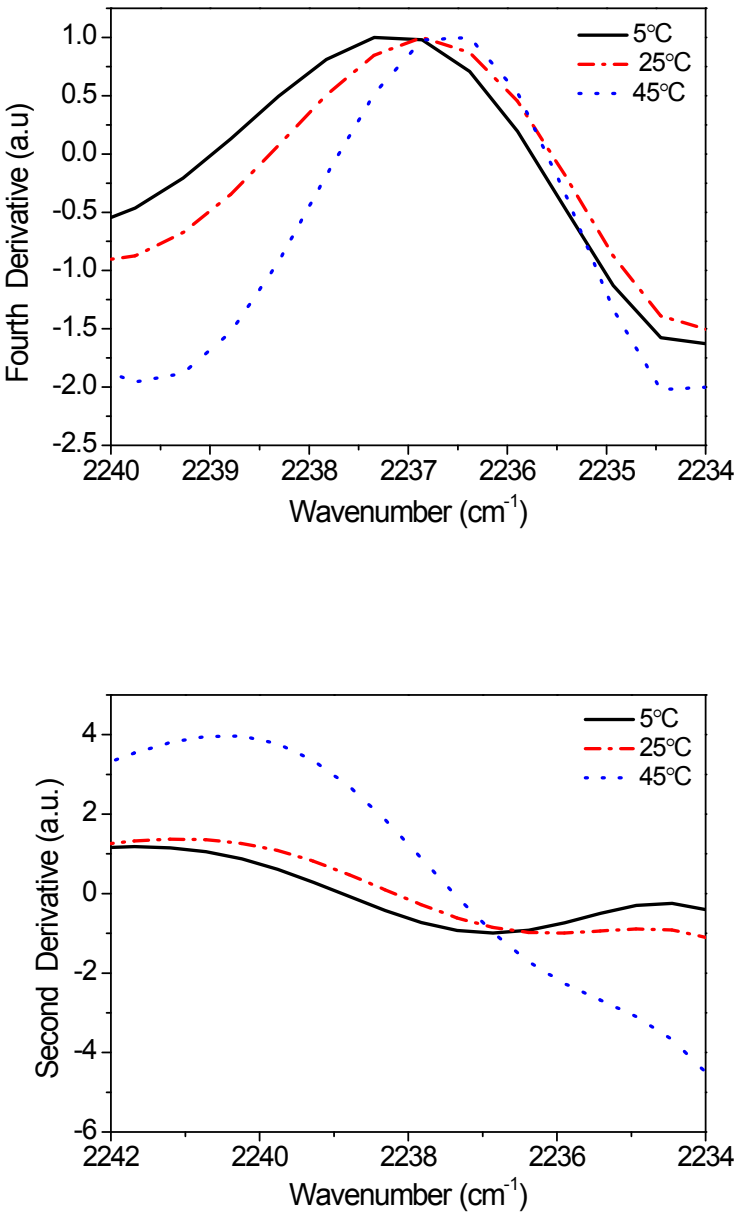

Figure S5. B) Temperature-dependent change of the derivative spectra of the CN stretch of *p*-tolunitrile in isopropanol. Top: fourth derivative spectra; Bottom: second derivative spectra.

Note: Fourth derivative technique is needed in order to more accurately extract the CN frequency in the second derivative spectrum. The fourth derivative spectrum was obtained by performing second derivative treatment twice on the absorption spectrum.

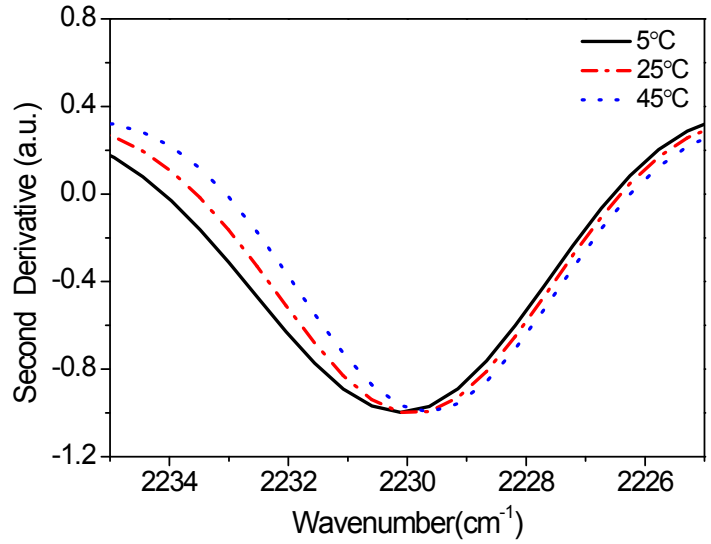

Figure S5. C) Temperature-dependent change of the second derivative spectra of the CN stretch of *p*-tolunitrile in formamide.

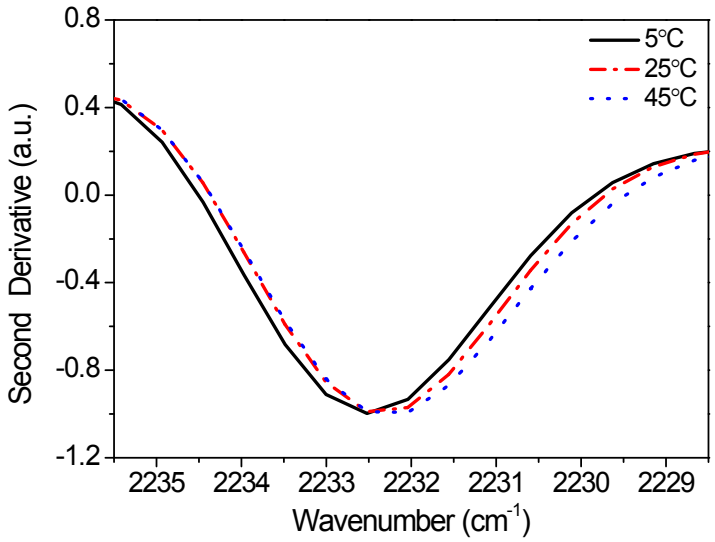

Figure S5. D) Temperature-dependent change of the second derivative spectra of the CN stretch of *p*-tolunitrile in cyclohexane.

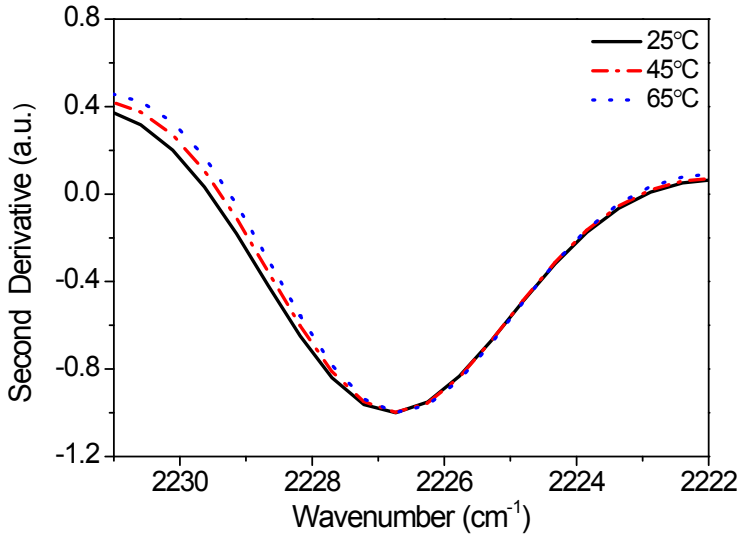

Figure S5. E) Temperature-dependent change of the second derivative spectra of the CN stretch of *p*-tolunitrile in DMSO.

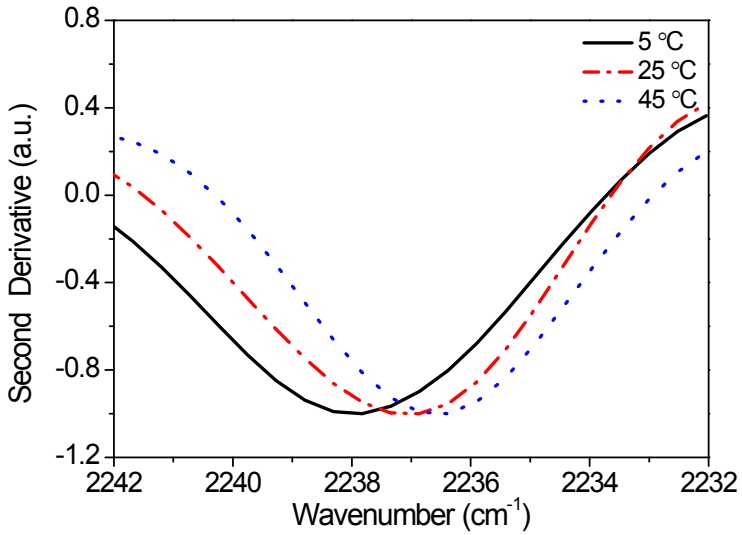

Figure S5. F) Temperature-dependent change of the second derivative spectra of the CN stretch of the KLVXFAK monomer in water (i.e., the 2237 cm^{-1} peak).

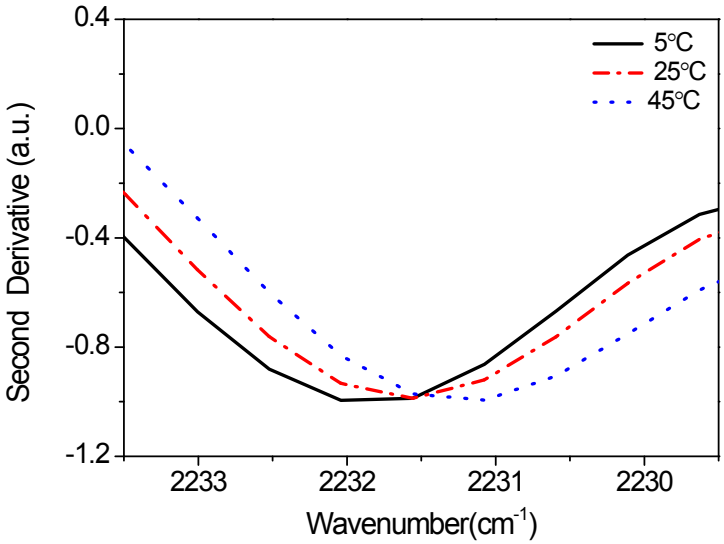

Figure S5. G) Temperature-dependent change of the second derivative spectra of the KLVXFAK nanosheet (i.e., the 2231 cm^{-1} peak).

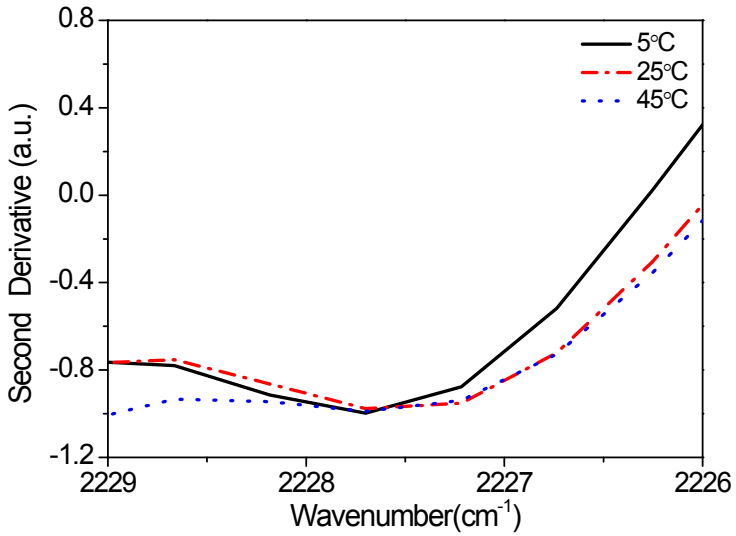

Figure S5. H) Temperature-dependent change of the second derivative spectra of the off-pathway KLVXFAK amorphous aggregate (i.e., the 2227 cm^{-1} peak).

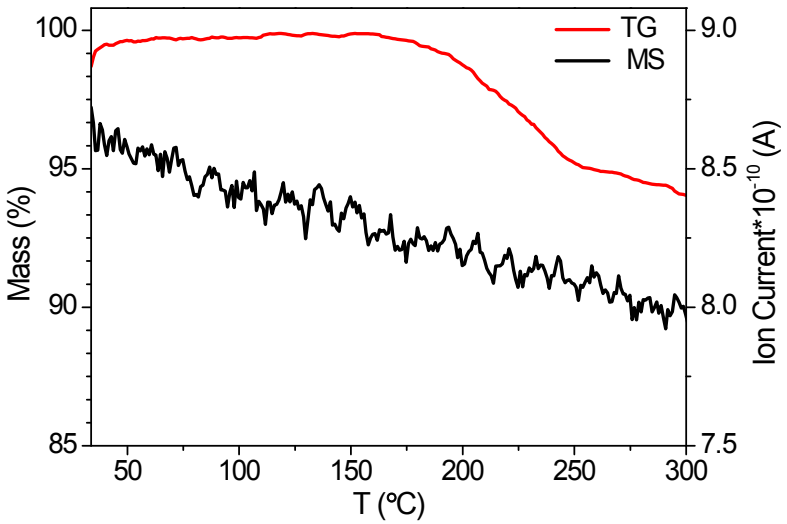

Figure S6. TG/MS curves of the KLVXFAK nanosheet.

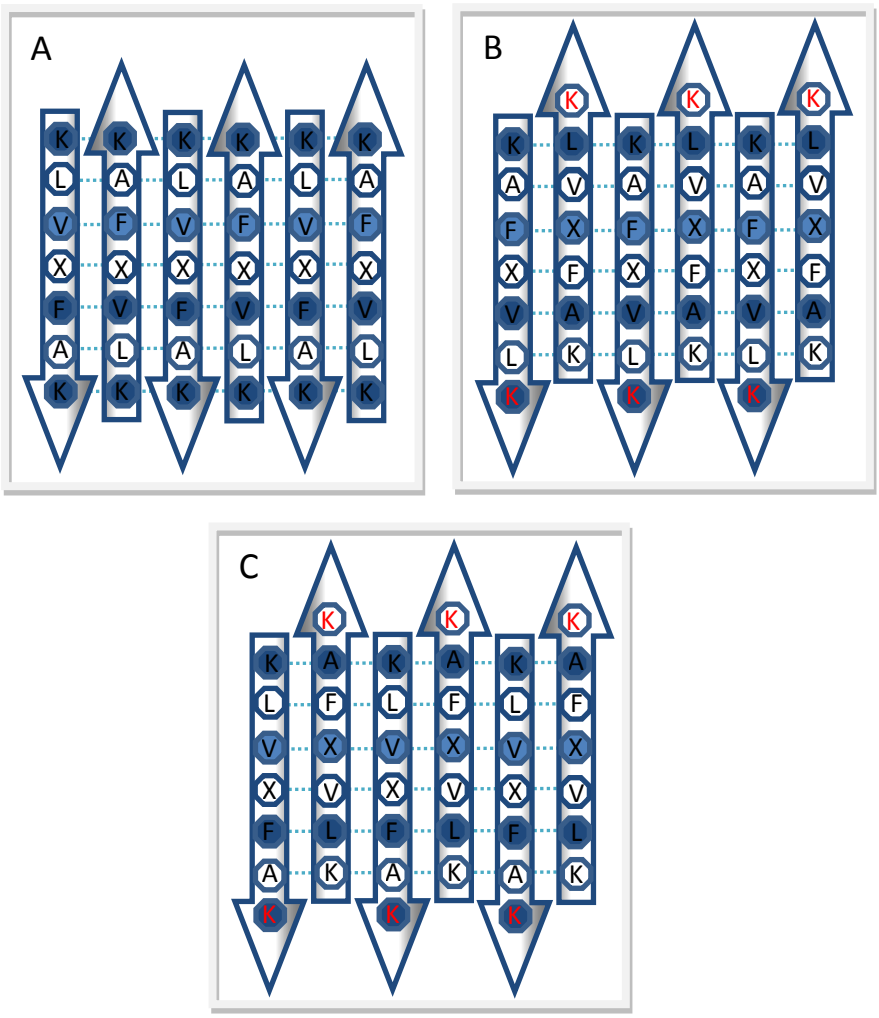

Figure S7. Three possible antiparallel β-sheet configurations by KLVXFAK strands. Each arrow represents an individual KLVXFAK β-strand (from N terminal to C terminal) and six strands are shown as representatives for each β-sheet. Octagon with letter: amino acid residue; shaded octagon: residue with its side chain pointing away from the viewer; open octagon: residue with its side chain pointing towards the viewer; red color K: dangling K.

Note: A and B configurations contain π-stacking structure. Namely, in A, the aromatic side chains of X are aligned in register; in B, the aromatic side chains of X and F are aligned in register. C configuration contains no π-stacking structure. Namely, in C, the aromatic side chains of X and the aliphatic side chains of V are aligned in register.

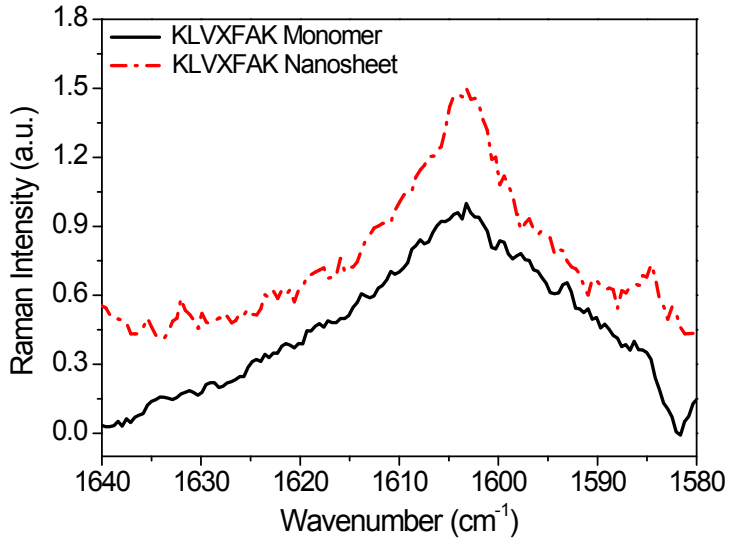

Figure S8. Comparison of the Raman spectra of the KLVXFAK monomer and the KLVXFAK nanosheet. The two spectra have been scaled and then offset vertically for better display. a.u.: arbitrary unit.

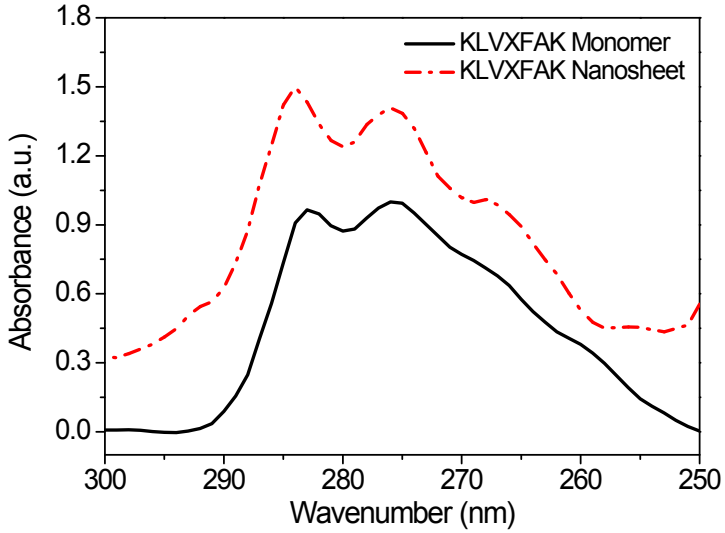

Figure S9. Comparison of the UV-Vis spectra of the KLVXFAK monomer and the KLVXFAK nanosheet. The nanosheet spectrum has been baseline corrected; the two spectra have been offset vertically for better display and their absorbance values are thus in arbitrary unit (a.u.).

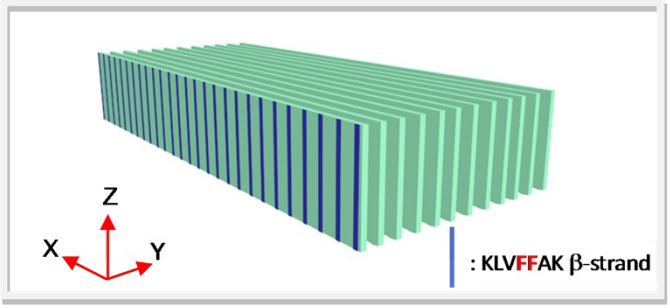

Figure S10. The hierarchical structural model for the KLVFFAK amyloid nanosheet proposed by Dai et al.[1] Each blue stripe represents an individual KLVFFAK β-strand and each green sheet represents an individual KLVFFAK β-sheet. These β-sheets stand perpendicular to the X-Y plane.

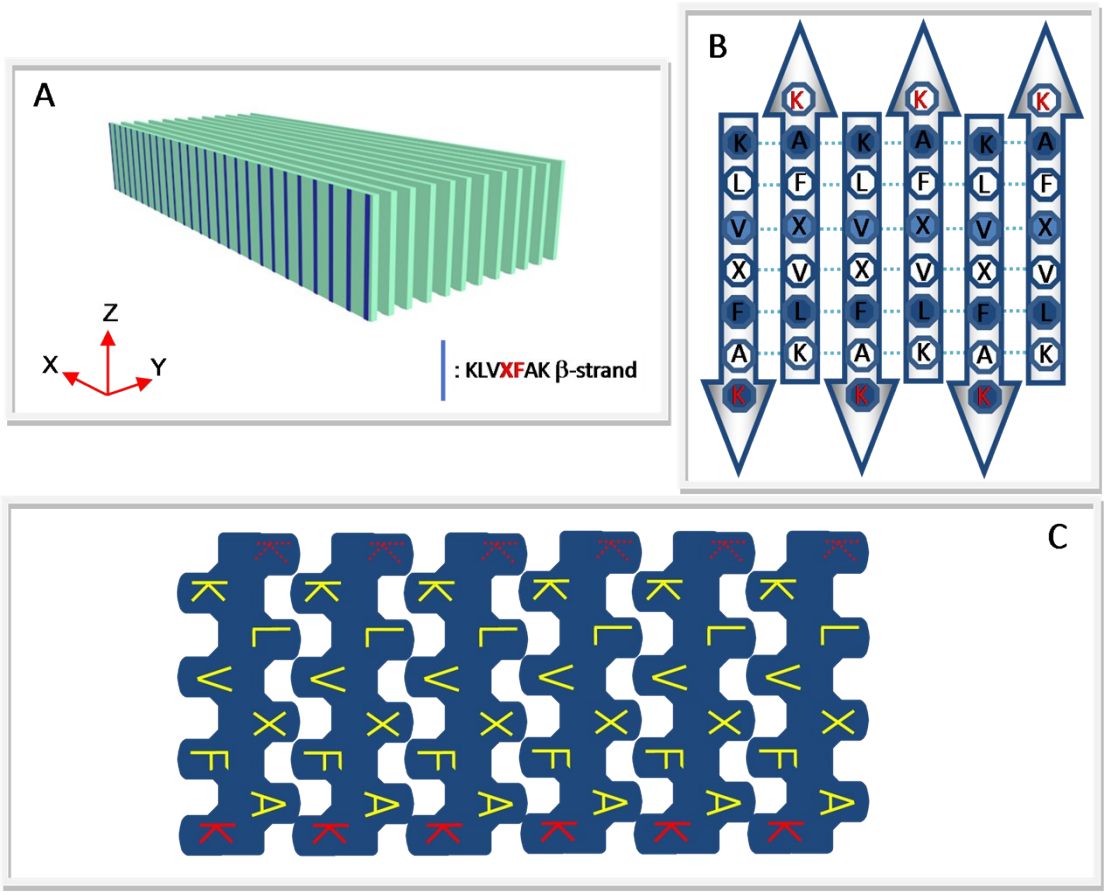

Figure S11. An alternative hierarchical structural model for the KLVXFAK amyloid nanosheet. A: Overview of the model. Each blue stripe represents an individual KLVXFAK β-strand and each green sheet represents an individual KLVXFAK antiparallel β-sheet. These β-sheets stand perpendicular to the X-Y plane. B: View towards the X-Z plane where the viewer can see the details of the KLVXFAK antiparallel β-sheet. Each arrow represents an individual KLVXFAK β-strand (from N terminal to C terminal) and six strands are shown as representatives. Octagon with letter: amino acid residue; shaded octagon: residue with its side chain pointing away from the viewer; open octagon: residue with its side chain pointing towards the viewer; red-color K: dangling K. C: View towards the Y-Z plane where the viewer can see the details of the steric-zipper-like structure. Each unit represents the view of the edge of the KLVXFAK β-sheet and six units are shown as representatives. The viewer can see all of the seven residues (K16, L17, V18, X19, F20, A21, and K22) from the front β-

strand and one dangling K22 from the second β-strand. Solid red-color K: dangling K from the front strand; dotted red-color K: dangling K from the second β-strand. Yellow color K, L, V, X, F, A are from the front β-strand; and underneath these displayed residues are those non-displayed residues from the second β-strand, which are A (under K), F (under L), X (under V), V (under X), L (under F), K (under A).

Note: In this model, there is no possibility for the CN probe of the X residue to form a H-bond with its neighboring residues, thus conflicting with our experimental observation that the CN probe is H-bonded with K.

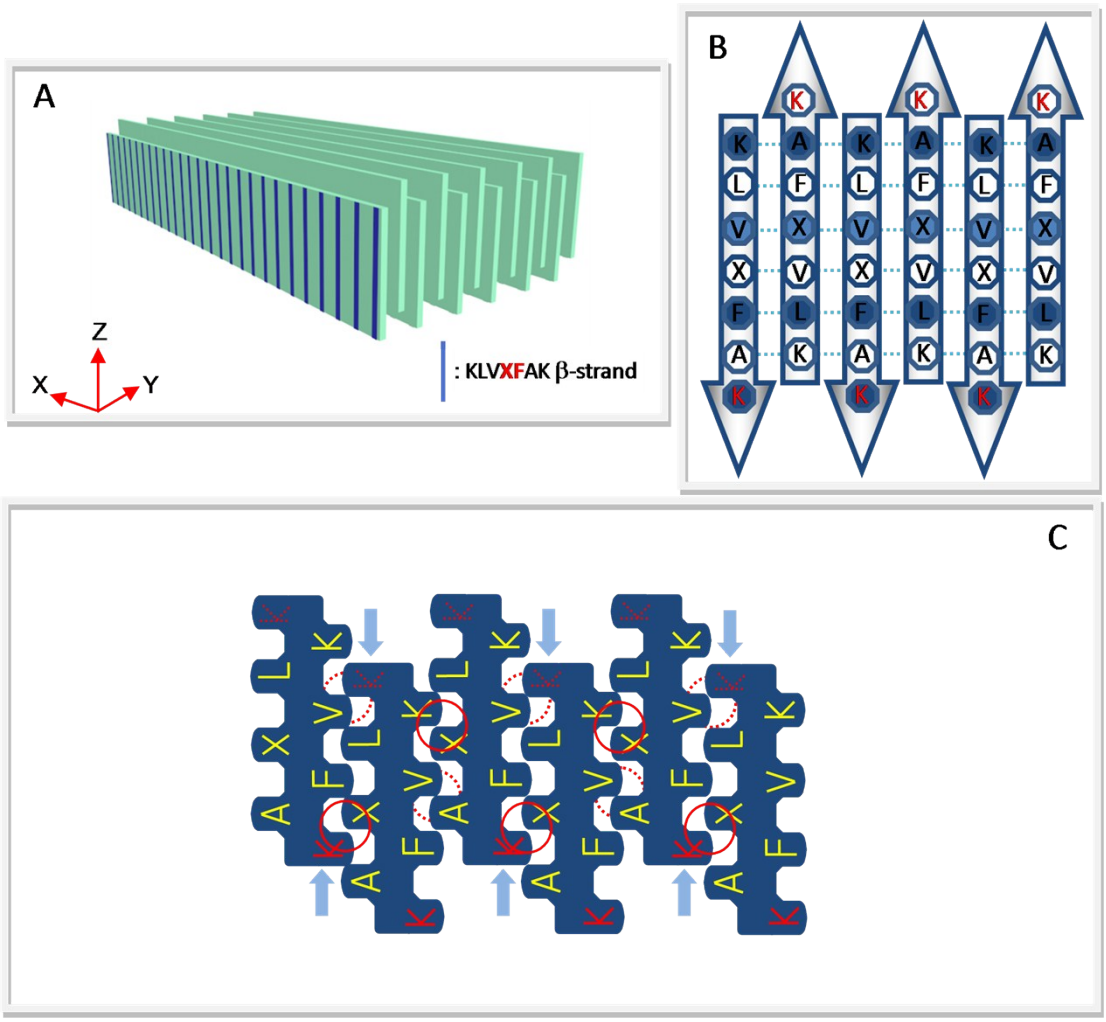

Figure S12. An alternative hierarchical structural model for the KLVXFAK amyloid nanosheet. (A) Overview of the model. Each blue stripe represents an individual KLVXFAK β-strand and each green sheet represents an individual KLVXFAK antiparallel β-sheet. These β-sheets stand perpendicular to the X-Y plane. (B) View towards the X-Z plane. Each arrow represents an individual KLVXFAK β-strand (from N terminal to C terminal) and six strands are shown as representatives; Octagon with letter: amino acid residue; shaded octagon: residue with its side chain pointing away from the viewer; open octagon: residue with its side chain pointing towards the viewer; red-color K: dangling K. (C) View towards the Y-Z plane where the viewer can see the details of the steric-zipper-like structure. Each unit represents the view of the edge of the KLVXFAK β-sheet and six units are shown as representatives. The viewer can see all of the seven residues (K16, L17, V18, X19,

F20, A21, and K22) from the front β-strand and one dangling K22 from the second β-strand. Solid red-color K: dangling K from the front strand; dotted-red color K: dangling K from the second β-strand. Yellow color K, L, V, X, F, A are from the front β-strand; and underneath these displayed residues are those non-displayed residues from the second β-strand, which are A (under K), F (under L), X (under V), V (under X), L (under F), K (under A). Solid red circle indicates the location of the H-bond between X and K; and dotted red circle indicates the location of the H-bond between X and K where X is underneath V. The light blue arrow indicates the location of water solvent exposure site.

Note: The difference of this model with the model in Figure 9 is that it allows the H-bonding formation between dangling K and CN. Yet, there are two reasons to exclude this model. First, with this model, the height of KLVXFAK nanosheet would be higher than that of the KLVFFAK nanosheet in Figure S10 by a three-residue-length which corresponds to about 1 nm. This conflicts with our AFM observation that the KLVXFAK and KLVFFAK nanosheets have similar heights. Second, since X is H-bonded by the dangling K, there are chances for X to be partially solvent exposed as the space underneath the dangling K (as indicated by the light blue arrows) can accommodate solvent water molecule. This would let us observe a CN frequency shift in the dehydration study. Yet, in our dehydration study (refer to Figure 7), after we dried the KLVXFAK nanosheet, we did not observe such frequency shift.

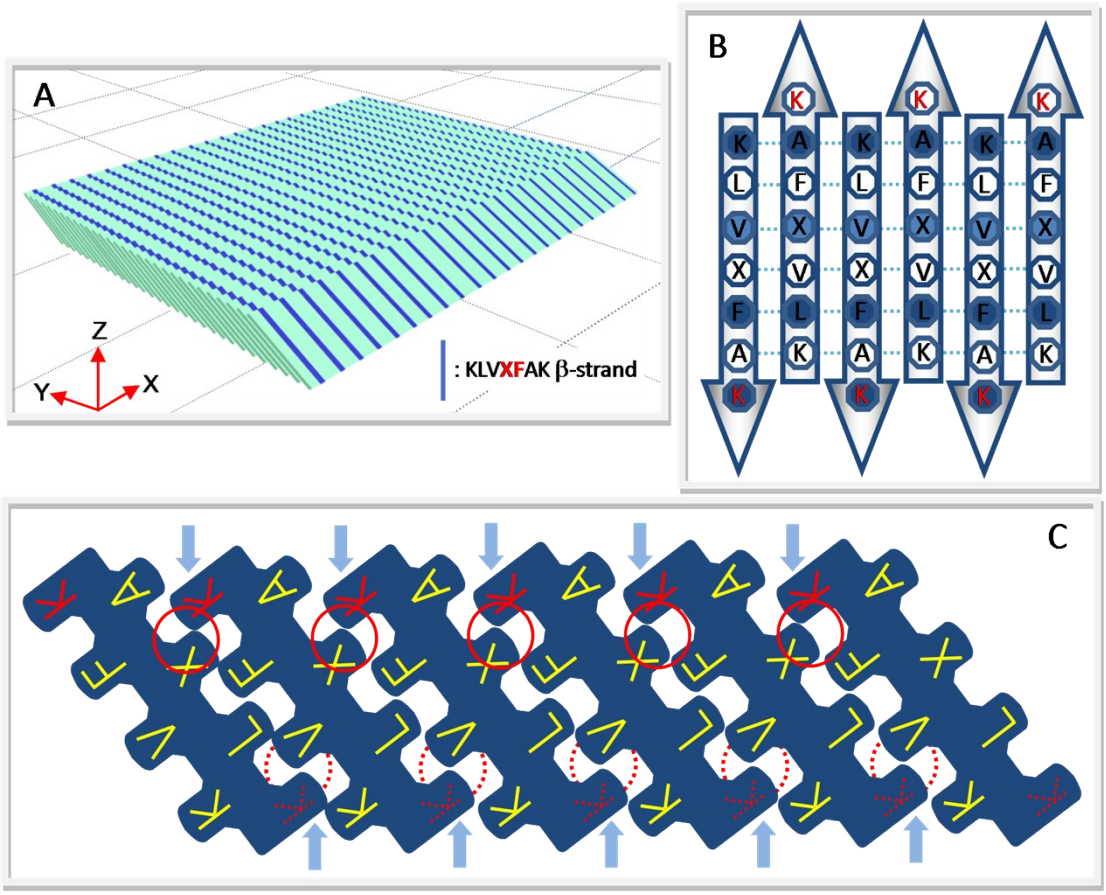

Figure S13. An alternative hierarchical structural model for the KLVXFAK amyloid nanosheet. A: Overview of the model. Each blue stripe represents an individual KLVXFAK β-strand and each green sheet represents an individual KLVXFAK antiparallel β-sheet. These β-sheets stand tilted relative to the X-Y plane. B: View towards the X-Z plane where the viewer can see the details of the KLVXFAK antiparallel β-sheet. Each arrow represents an individual KLVXFAK β-strand (from N terminal to C terminal) and six strands are shown as representatives. Octagon with letter: amino acid residue; shaded octagon: residue with its side chain pointing away from the viewer; open octagon: residue with its side chain pointing towards the viewer; red-color K: dangling K. C: View towards the Y-Z plane where the viewer can see the details of the steric-zipper-like structure. Each unit represents the view of the edge of the KLVXFAK β-sheet and six units are shown as representatives. The viewer can see all of the seven residues (K16, L17, V18, X19, F20, A21, and K22) from the front β-strand and one dangling K22 from the second β-strand. Solid red-color K: dangling K

from the front strand; dotted red-color K: dangling K from the second β-strand. Yellow color K, L, V, X, F, A are from the front β-strand; and underneath these displayed residues are those non-displayed residues from the second β-strand, which are A (under K), F (under L), X (under V), V (under X), L (under F), K (under A). Solid red circle indicates the location of the H-bond between X and K; and dotted red circle indicates the location of the H-bond between X and K where X is underneath V. The light blue arrow indicates the location of water solvent exposure site.

Note: The difference of this model with the model in Figure 9 is that it allows the H-bonding formation between dangling K and CN. Since X is H-bonded by the dangling K, there are chances for X to be partially solvent exposed as the space underneath the dangling K (as indicated by the light blue arrows) can accommodate solvent water molecule. This would let us observe a CN frequency shift in the dehydration study. Yet, in our dehydration study (refer to Figure 7), after we dried the KLVXFAK nanosheet, we did not observe such frequency shift.

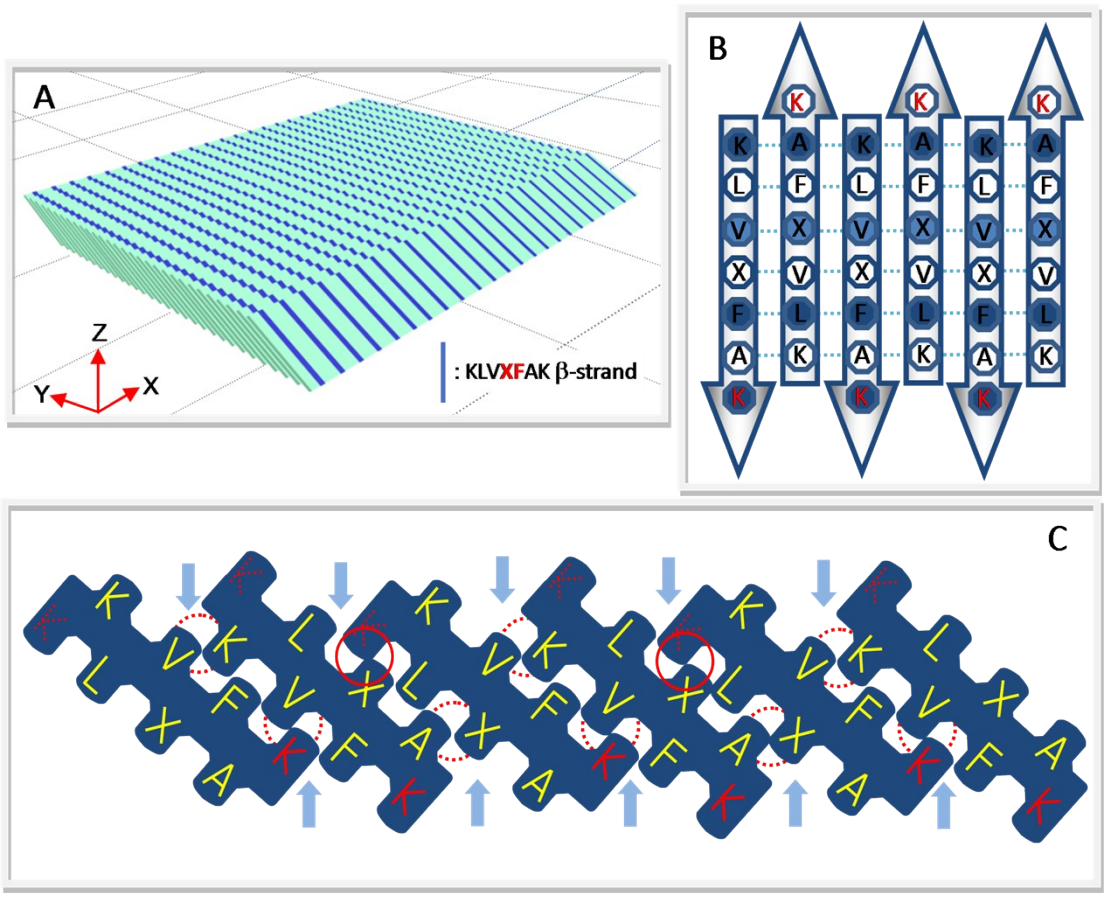

Figure S14. An alternative hierarchical structural model for the KLVXFAK amyloid nanosheet. A: Overview of the model. Each blue stripe represents an individual KLVXFAK β-strand and each green sheet represents an individual KLVXFAK antiparallel β-sheet. These β-sheets stand tilted relative to X-Y plane. B: View towards the X-Z plane where the viewer can see the details of the KLVXFAK antiparallel β-sheet. Each arrow represents an individual KLVXFAK β-strand (from N terminal to C terminal) and six strands are shown as representatives. Octagon with letter: amino acid residue; shaded octagon: residue with its side chain pointing away from the viewer; open octagon: residue with its side chain pointing towards the viewer; red-color K: dangling K. C: View towards the Y-Z plane where the viewer can see the details of the steric-zipper-like structure. Each unit represents the edge view of the KLVXFAK β-sheet and six units are shown as representatives. Unlike in the structural model shown in Figure 9 where the six units are identical, here each unit is

rotated by 180° relative to its neighboring unit within the β-sheet plane. This configuration makes the steric-zipper class to be class 8. The viewer can see all of the seven residues (K16, L17, V18, X19, F20, A21, and K22) from the front β-strand and one dangling K22 from the second β-strand. Solid red-color K: dangling K from the front strand; dotted red-color K: dangling K from the second β-strand. Yellow color K, L, V, X, F, A are from the front β-strand; and underneath these displayed residues are those non-displayed residues from the second β-strand, which are A (under K), F (under L), X (under V), V (under X), L (under F), K (under A). Solid red circle indicates the location of the H-bond between X and K; and dotted red circle indicates the location of the H-bond between X and K where X is underneath V. The light blue arrow indicates the location of water solvent exposure site.

Note: This model contains class 8 type steric zipper. According to Eisenberg's definition,[2] for the two β-sheets in a class 8 steric zipper, the up-and-down orientation of the two sheets are opposite. This model conflicts with the observation in the dehydration study. As indicated by the light blue arrows, X (either displayed or underneath V) in these locations can be solvent exposed. This would let us observe a CN frequency shift in the dehydration study. Yet, in our dehydration study (refer to Figure 7), after we dried the KLVXFAK nanosheet, we did not observe such frequency shift.

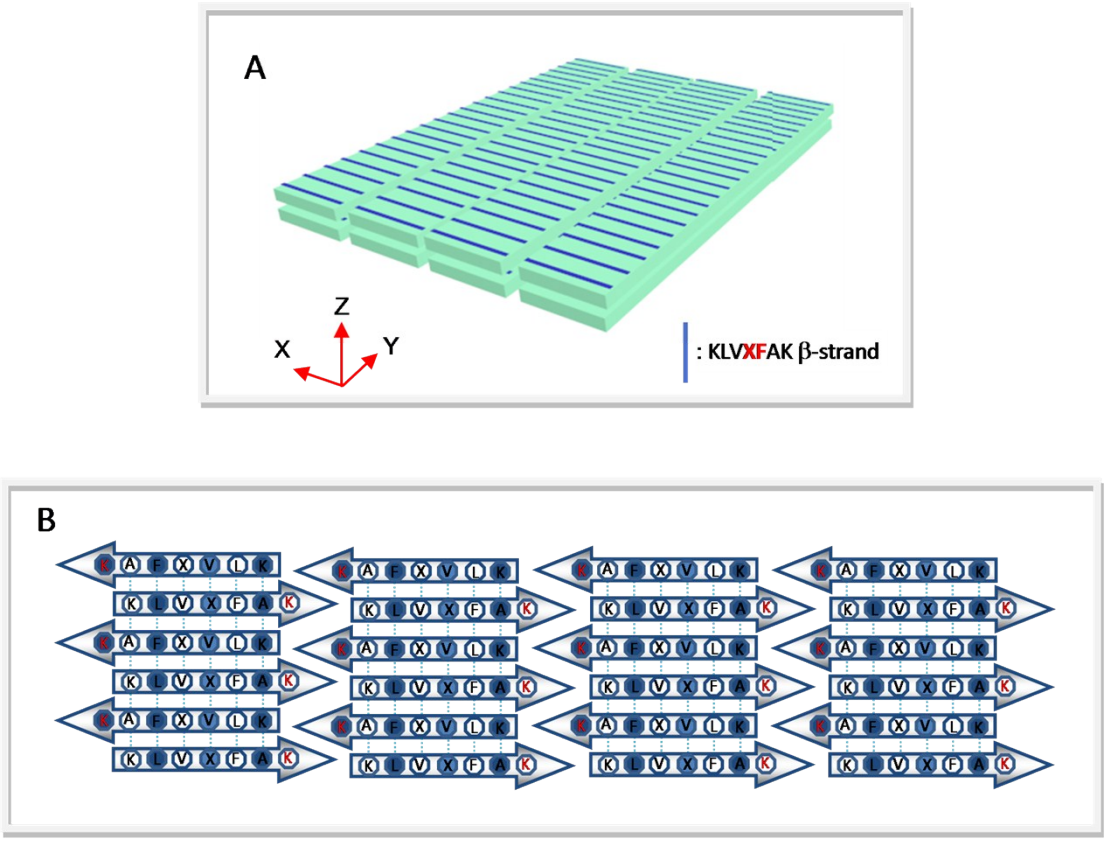

Figure S15. An alternative hierarchical structural model for KLVXFAK amyloid nanosheet. A: Overview of the model. Each blue stripe represents an individual KLVXFAK β-strand and each green sheet represents an individual KLVXFAK antiparallel β-sheet. Each pair of β-sheets constitutes an amyloid fibril. There are a total of four fibrils shown as representatives here. Unlike the model proposed in Figure 9 where the KLVXFAK β-strands "stand tilted" relative to the X-Y plane, in this model the KLVXFAK β-strands lie flat on top of the X-Y plane. (B) Top view of the model (towards the X-Y plane). Each arrow represents an individual KLVXFAK β-strand (from N terminal to C terminal) and 24 strands in four β-sheets are shown as representatives. Octagon with letter: amino acid residue; shaded octagon: residue with its side chain pointing away from the viewer; open octagon: residue with its side chain pointing towards the viewer; red-color K: dangling K.

Note: This nanosheet structure is formed by lateral association of individual KLVXFAK amyloid fibrils through the interaction between their N terminals and C

terminals. This type of amyloid assembly has been proposed by Mezzenga and coworkers recently to explain the structure of some giant amyloid ribbons.[3, 4] As the thickness of a single β-sheet is about 1 nm,[5] the thickness of the nanosheet in Figure S15A would be about 2 nm. This is approximately consistent with our AFM height observation. Yet, this model conflicts with the observation in the dehydration study. As we can see from the top view of the nanosheet in Figure S15B, with our proposed antiparallel β-sheet configuration, there are always some X residues (i.e., open octagons) pointing to the solvent with its CN probe exposed to water. Dehydration process would make these solvent-exposed CN probes change their status from being hydrated to being dehydrated. Correspondingly, the CN frequency of X residue should experience some shift. Yet, in our dehydration study (refer to Figure 7), after we dried the KLVXFAK nanosheet, we did not observe such frequency shift.

Reference

1. B. Dai, D. Li, W. Xi, F. Luo, X. Zhang, M. Zou, M. Cao, J. Hu, W. Y. Wang, G. H. Wei, Y. Zhang and C. Liu, *Proc. Natl. Acad. Sci. U. S. A.*, 2015, **112**, 2996-3001.
2. M. R. Sawaya, S. Sambashivan, R. Nelson, M. I. Ivanova, S. A. Sievers, M. I. Apostol, M. J. Thompson, M. Balbirnie, J. J. W. Wiltzius, H. T. McFarlane, A. O. Madsen, C. Riekel and D. Eisenberg, *Nature*, 2007, **447**, 453-457.
3. C. Lara, J. Adamcik, S. Jordens and R. Mezzenga, *Biomacromolecules*, 2011, **12**, 1868-1875.
4. C. Lara, N. P. Reynolds, J. T. Berryman, A. Xu, A. Zhang and R. Mezzenga, *J. Am. Chem. Soc.*, 2014, **136**, 4732-4739.
5. M. S. Lamm, K. Rajagopal, J. P. Schneider and D. J. Pochan, *J. Am. Chem. Soc.*, 2005, **127**, 16692-16700.